



Effective properties of a new auxetic triangular lattice: an analytical approach

L. Cabras

Università degli Studi di Cagliari, Dipartimento di Ingegneria Civile, Ambientale e Architettura
luigi.cabras@unica.it

M. Brun

Università degli Studi di Cagliari, Dipartimento di Ingegneria Meccanica, Chimica e dei Materiali;
University of Liverpool, Department of Mathematical Sciences
mbrun@unica.it

ABSTRACT. In this article we propose a new auxetic periodic lattice with negative Poisson's ratio which tends to the limit $\nu=-1$ under particular conditions. We have studied its generation and kinematic, and we give a full description of the mechanical properties of this innovative model. Calibrating the geometrical configuration of the lattice and the mechanical properties of the constituent material we are able to have a Poisson's ratio which is arbitrarily close to -1.

KEYWORDS. Auxetic lattice; Negative Poisson's ratio; Mechanical properties.

INTRODUCTION

Poisson's Ratio, usually represented by ν , is defined as the ratio of transverse contraction strain to longitudinal extension strain with respect to the direction of stretching force applied. Since tensile deformation is considered positive and compressive deformation is considered negative in the definition of Poisson's ratio is introduced a minus sign, so that common materials have a positive ratio. However, there are particular materials that expand laterally when stretched longitudinally with a negative Poisson's ratio, they were named for the first time auxetic materials by Ken Evans in an article in *Nature* (1991). For isotropic materials it may be shown that Poisson's ratio is between $-1 \leq \nu \leq 1/2$ in 3D and $-1 \leq \nu \leq 1$ in 2D, for anisotropic materials ν is not restricted by the above limits. The value of the Poisson's ratio has also important consequences for other aspects of the behavior of materials, in fact the most materials resist a change in volume as determined by the bulk modulus K more than they resist a change in shape, as determined by the shear modulus μ , the values of K are typically larger than the values of μ . By changing the microstructure of a material in such a way that the Poisson's ratio ν is lower, the values of K and μ can be altered. Decreasing the value of ν to negative value, it would result into a material with a higher shear modulus μ than the bulk modulus K . Different geometrical structures and models are created trying to reproduce some observed feature in auxetic materials, ranging from the macroscopic to microscopic and to the molecular levels. A simple classification can be based on mechanical considerations. Almost all of these models are based on a simple mechanism that is treated as a unit cell leading to a global stiffening effect. One of the earliest models used to describe these special materials was that with re-entrant structure, firstly suggested in [1]. Over the years, many more sophisticated models have been proposed. Another model is based on chiral structure, the researchers in this area use the adjective "chiral" to mean a physical property of spinning. In this type of structures, basic chiral units

are firstly formed by connecting straight ligaments to central nodes which may be circles or rectangles or other geometrical forms. The auxetic effects are achieved through wrapping or unwrapping of the ligaments around the nodes in response to an applied force, as shown in [2], the Poisson's ratio ν of a chiral structure for in-plane deformations, with flexible ribs and rigid node, can be tailored to be around -1. Later Ruzzene and Spadoni, in [3], have considered the behavior of structures by introducing the flexibility of the nodes.

Other models, as in [4], derive the auxetic behavior by the rotation of rigid or semi-rigid shapes (triangle, squares, rectangles and tetrahedron) when loaded, this type of structures has been developed to reproduce the behavior of foams and hypothetical nanostructure networked polymers. A different approach is followed by Bathurst and Rothenburg in [5], they formulate the incremental response of an assembly of elastic spheres, considering an isotropic distribution of contacts around a particle. Since the negative Poisson's ratio is a scale independent property the auxetic behavior can be achieved at a macroscopic or microstructural level, or even at the mesoscopic and molecular levels, many models were developed to simulate polymeric structure or anisotropic fibrous composites. The first auxetic microporous polymeric material was investigated in [6]. It was an expanded foam of PTFE which has a highly anisotropic negative $\nu = -12$. Several cases of negative Poisson's ratios have been discovered in the analysis of anisotropic fibrous composites. In these composites there is a high degree of anisotropy and the negative Poisson's ratio only occurs in some directions; in some cases only over a narrow range of orientation angle between the applied load and the fibers. In a recent advance, laminate structures have been presented which give rise to intentional negative Poisson's ratios combined with mechanical isotropy in two dimensions or in three dimensions. These laminates have structure on several levels of scale; they are hierarchical. By appropriate choice of constituent properties one can achieve Poisson's ratios approaching the lower limit of -1.

Auxetic systems perform better than classical material in a number of applications, due to their superior properties. They have been shown to provide better indentation resistance [7, 8 and 9] for their property of “densification” in the vicinity of an impact. The auxetic materials form dome shaped structures [10, 11] when they are subjected to out of plane bending moments instead the saddle shape adopted by the common materials. Also, they can be useful when we need better acoustic and vibration properties than the conventional materials [12, 13 and 14].

MODEL OF PERIODIC LATTICE WITH AUXETIC MACROSCOPIC BEHAVIOR

We consider radially foldable structure formed by two angulated elements ABC and DBE, shown in Fig. 1, connected together through a hinge in B.

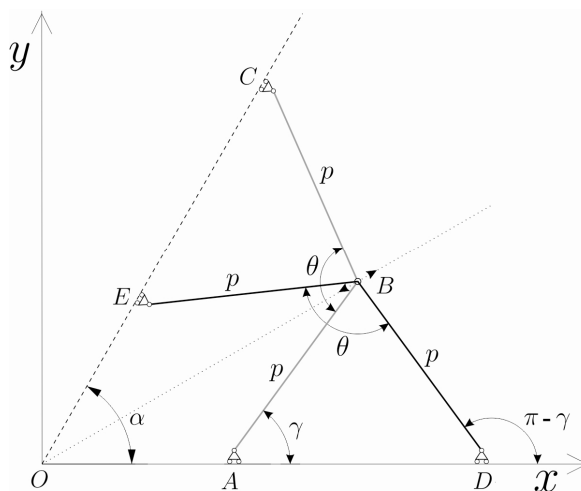


Figure 1: Pair of linkages movable with a single degree of freedom. The two rigid linkages ABC and EBD are shown in grey and black, respectively. They are constraint at the “coupler” point B to have the same displacement components. Points A and D and E and C can only move along straight lines.

The coupled angulated elements ABC and DBE can roto-translate with a single degree of freedom and the end point A, C, D and E can only translate along to Ox-axis and the axis inclined by the angle α with respect to the Ox-axis, respectively.



In analyzing the trajectory of the central point B, we also follow the more general formulation given in [15]. In Fig. 1, p is the length of the arms, θ the internal angle between them and α is the angle between the two straight lines along which the points A, D and C, E are constrained to move. B is the “coupler” point of the linkage. The equation for the one-parameter trajectory followed by the point B is obtained fixing the values of the geometric variables p , θ , α ; then, the position of B is determined by the angle γ . When we couple the movement of the linkage ABC with the linkage EBD, we obtain a relation between angles θ and α . The common point B follows the radial line OB:

$$y = \frac{\sin\theta}{1 - \cos\theta} x \quad (1)$$

The two linkages are assembled in order to create a radially foldable structure, as depicted in Fig. 2 and to avoid crossover with other pairs in a polar arrangement of the fully radially foldable structure the angle γ has to satisfy the bound

$$\alpha - \eta = \gamma = \pi - \eta, \quad (2)$$

where $\eta = \widehat{BAC} = \widehat{BDE}$. Different configurations are shown in Fig. 2b; the point B for each pair of linkages moves radially and the corresponding Poisson's ratios is equal to -1. We consider the triangular geometries with $\alpha = 2\pi/3$.

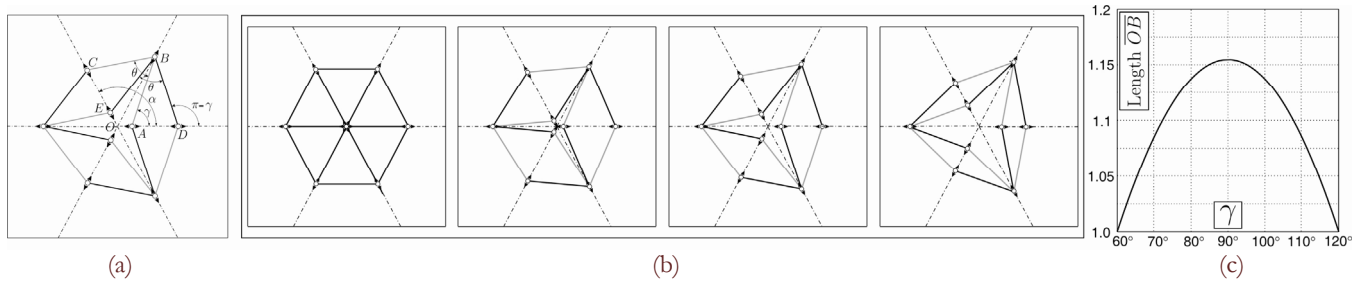


Figure 2: (a) Radially foldable structure with geometric parameters. (b) Configurations of the single degree of freedom lattices at different values of the geometrical parameter. (c) The radial distance OB as a function of γ is also given for $p=1$.

Construction of periodic lattice

The kinematically compatible periodic structures shown in Fig. 3 is obtained by a periodic distribution of the single cell elements shown in Fig. 2 as in [16].

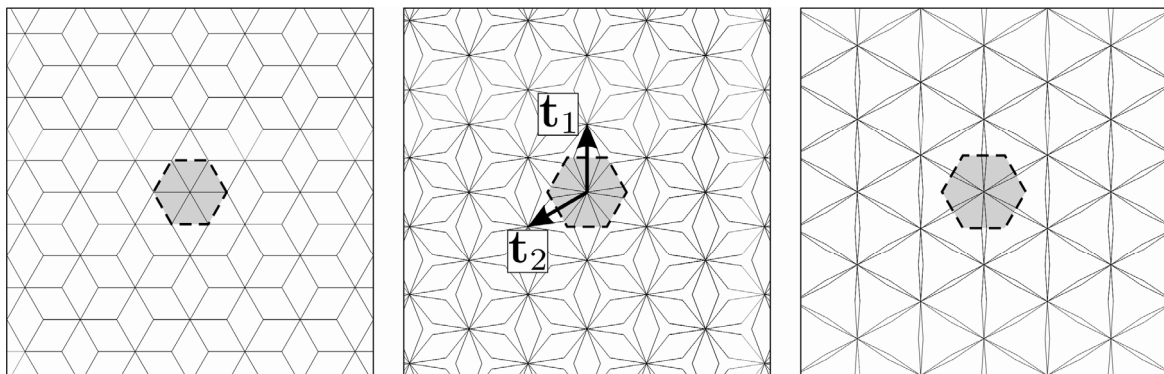


Figure 3: Periodic microstructure. Three different configurations, for different values of α are shown. The grey dashed region is the unit cell of the Bravais lattice where t_1 and t_2 are the primitive vectors.

The microstructure is composed of shaped elements with 12 arms of the same length. A system of cross couple is built where two elements are disposed in two different planes. Each cross couple is mutually constrained to have the same displacement at the central point where a hinge is introduced. Different couples of crosses are then constrained each other by internal hinges at the external end of each arm. The periodic structures have a Bravais periodic lattice [17] consisting of points:

$$\mathbf{R} = n_1 \mathbf{t}_1 + n_2 \mathbf{t}_2 \quad (3)$$

where $n_{1,2}$ are integers and $\mathbf{t}_{1,2}$ the primitive vectors spanning the lattice.

EFFECTIVE PROPERTIES OF THE PERIODIC AUXETIC LATTICE

Macroscopic properties are derived analytically for our lattice. The triangular lattice have three-fold symmetries and basic considerations on the symmetry group of the material lead to the conclusion that its constitutive behavior is isotropic (in the plane of deformation). Therefore, it will be necessary to compute two effective elastic constants. Stability constraints the in-plane Poisson's ratio to range between -1 and 1. Effective properties are denoted as K^* (bulk modulus), E^* (Young's modulus), μ^* (shear modulus) and ν^* (Poisson's ratio) and macroscopic stress and strain as $\bar{\sigma}$ and $\bar{\epsilon}$, respectively. The structure is composed of slender crosses and classical structural theories can be conveniently applied to analyze the response of the elastic system. In particular, each arm of a single cross is modeled as an Euler beam undergoing flexural and extensional deformations. Each beam have Young's modulus E , cross-sectional area A and second moment of inertia J . Additional springs have longitudinal stiffness equal to k_L or rotational stiffness equal to k_R (see Fig. 4). We also introduce the non-dimensional stiffness ratio parameters $\alpha_1=k_L p/(EA)$, $\alpha_2=k_L p^3/(EJ)$, $\alpha_3=k_R/(pEA)$ and $\alpha_4=k_R p/(EJ)$.

Macroscopic stresses are computed averaging the resultant forces on the boundary of the unit cell. Periodic boundary condition have been applied on the boundary of the unit cell so that displacements are periodic and forces are anti-periodic. Additional constrains are introduced to prevent rigid body motions. To solve the structure we apply the Principle of Virtual Work (PVW). It states that, if a structure is in equilibrium, then, for any arbitrary small virtual displacement satisfying kinematic boundary conditions, the work done by the external forces must equal the work done by the internal forces. In the following, we apply the PVW in two steps: in the first we find the internal actions (bending moments M , axial forces P and spring forces S^L or moments M^R) of the structure searching for the kinematic admissible configuration in the set of statically admissible ones (Flexibility Method) and in the second step we compute the macroscopic displacements.

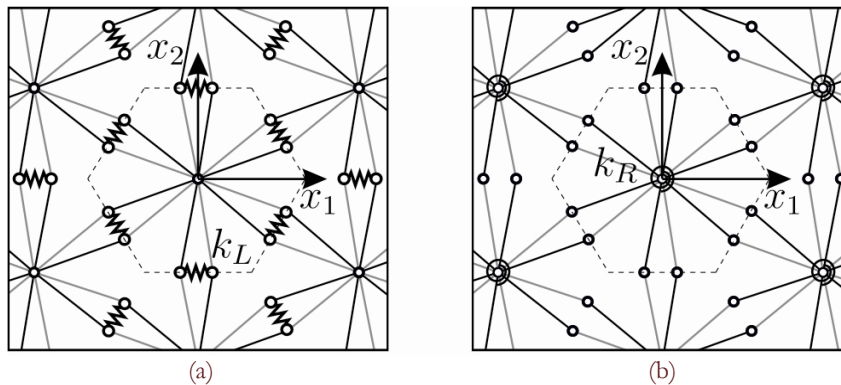


Figure 4: Lattice reinforced with elastic springs. (a) Longitudinal springs of stiffness k_L . (b) Rotational spring of stiffness k_R . The dashed contour indicates a typical unit cell of the periodic elastic system.

This procedure has the advantage to maintain the analytical treatment sufficiently simple. We point out that all the results have been also verified numerically implementing a finite element code in Comsol Multiphysics®. We consider the elastic structure as in Fig. 5a, subjected to normal and tangential external forces supposed to be known and corresponding to a macroscopic stress having components $\bar{\sigma}_{11}$ and $\bar{\sigma}_{22}$ different from zero. We define an equivalent statically determined system disconnecting two springs and introducing the dual static parameter as unknown X , equal for the two springs, as shown in Fig. 5b. Then, the general field of tension Ξ ($\Xi=M, N, S^L$ or M^R) in equilibrium with the external loads is:

$$\Xi = \Xi_0 + X\Xi_1 \quad (7)$$

where Ξ_0 is the solution of the static scheme in equilibrium with the external loads and $X=0$; while the field Ξ_1 is the solution of the static scheme in equilibrium with zero external loads and $X=1$. The deformed configurations of the isostatic equivalent structure violate the internal constraint in the two springs suppressed in the structure made isostatic.

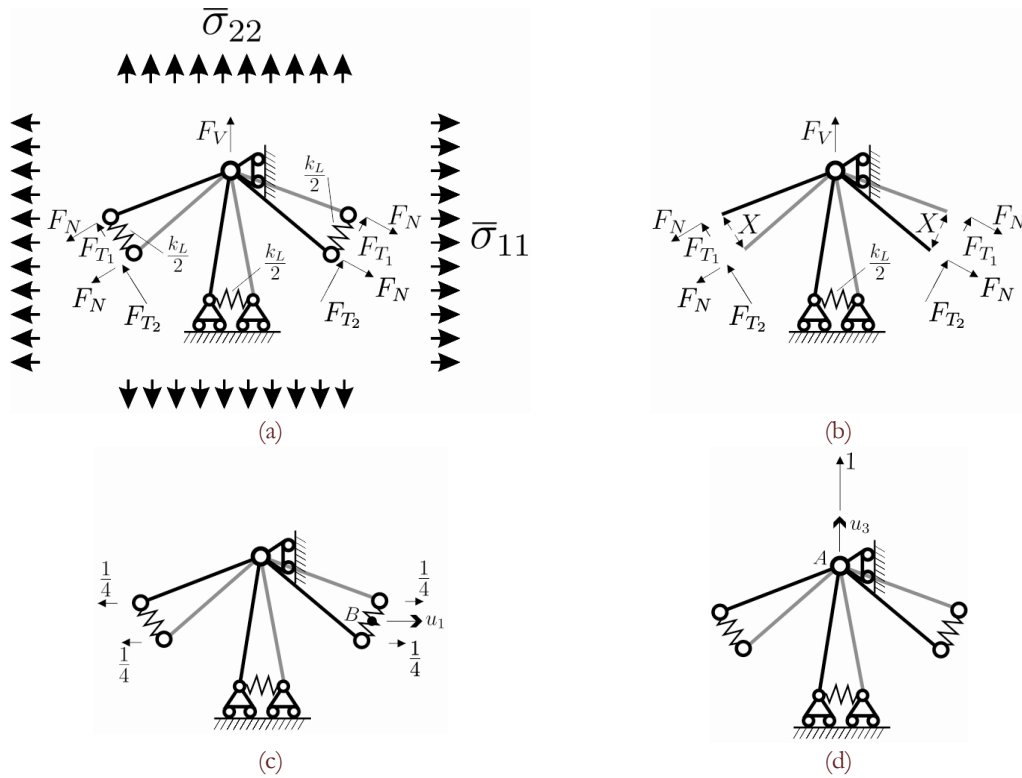


Figure 5: Application of the Principle of Virtual Displacements. Lattice reinforced with longitudinal springs. (a) Simplified structured analyzed for the computation of the effective properties. The applied forces F_N , F_V , F_{T1} and F_{T2} correspond to macroscopic stresses components. (b) Disconnected statically determined structure introduced for the determination of the internal actions (M,N, S^L). (c-d) Statically determined structure adopted for the computation of the displacement of the points A and B.

Such kinematic constraints must be restored imposing the kinematic compatibility equation that determines the values of the unknown X and uniquely defines the elastic solution of the problem, as follows:

$$X = - \frac{\sum_{\text{beam}} \int_0^l (M_0 \frac{M_1}{EJ} + N_0 \frac{N_1}{EA}) d\xi + \sum_{\text{spring}} S_0^L \frac{S_1^L}{k_L/2}}{\sum_{\text{beam}} \int_0^l (M_1 \frac{M_1}{EJ} + N_1 \frac{N_1}{EA}) d\xi + \sum_{\text{spring}} S_1^L \frac{S_1^L}{k_L/2}} = \left(\frac{F_N [(3\cos^2 \gamma - 1)\alpha_1 + \sin^2 \gamma \alpha_2 + 2] + F_V (\alpha_1 + 1)}{\sin^2 \gamma \alpha_2 + 3\cos^2 \gamma \alpha_1 + 3} \right) \cot \gamma \quad (8)$$

We note that for sufficiently slender beam structures, the contribution due to the shear deformation is negligible compared to that due to flexural and axial deformations and, therefore, it has been neglected.

We reconstruct the distribution of internal actions by a linear combination of partial diagrams of N and M and of the spring forces S^L , as functions of external forces F_N , $F_T = (F_{T1} + F_{T2})/2$ and F_V :

$$\begin{cases} N = N_0 + X N_1 \\ M = M_0 + X M_1 \\ S^L = S_0^L + X S_1^L \end{cases} \quad (9)$$

Applying a second time the PVW we calculate the displacement of the point A and B (center of the spring) as shown in Fig. 5c-5d. To do this we consider as kinematically admissible structure the real structure and as statically admissible structure, an isostatic structure subjected to horizontal and vertical forces of magnitude equal 1/4, respectively, so that the virtual external works coincide exactly with the horizontal and vertical displacement of the point B (u_1 and u_2 in Fig. 5c), and we calculate the displacement of the point A (u_3 in Fig. 5d) considering a vertical forces of unitary magnitude, so that the virtual external works coincide exactly with the vertical displacement of the point A. In particular the PVW equations have the form:



$$u_i = \sum_{\text{beam}} \int_0^l \left(M_i^* \frac{M}{EJ} + N_i^* \frac{N}{EA} \right) d\xi + \sum_{\text{spring}} S_i^{L*} \frac{S^L}{k_L/2}, \quad (i=1, 2 \text{ and } 3), \quad (10)$$

where M_i^* , N_i^* and S_i^{L*} (with $i=1, 2$ and 3) are the internal actions of the statically admissible structures subjected to forces applied in the point B in horizontal and vertical direction, and the internal actions of the statically admissible structure subjected to a vertical forces applied in the point A in vertical direction. The corresponding displacement are:

$$u_1 = A_1 F_N + B_1 F_T + C_1 F_V \quad u_2 = A_2 F_N + B_2 F_T + C_2 F_V \quad u_3 = A_3 F_N + B_3 F_T + C_3 F_V \quad (11)$$

where A_{1-3} , B_{1-3} , C_{1-3} are coefficients arising from the integrations. Previous equations are explicit linear relations between the forces F_N , F_T and F_V associated to macroscopic stresses

$$\begin{aligned} \bar{\sigma}_{11} &= \frac{\sqrt{3}F_N - F_T}{p \sin \gamma} \\ \bar{\sigma}_{22} &= \frac{4F_V + 2\sqrt{3}F_T + 2F_N}{2\sqrt{3}p \sin \gamma} \end{aligned} \quad (12)$$

and the displacements of the points A and B associated to macroscopic strains:

$$\begin{aligned} \bar{\epsilon}_{11} &= \frac{2u_1}{\sqrt{3}p \sin \gamma} = 2 \frac{A_1 F_N + B_1 F_T + C_1 F_V}{\sqrt{3}p \sin \gamma} \\ \bar{\epsilon}_{22} &= \frac{u_3}{p \sin \gamma} = 2 \frac{A_3 F_N + B_3 F_T + C_3 F_V}{p \sin \gamma} \end{aligned} \quad (13)$$

Solving previous relations (13) in term of F_N , F_T , and F_V and substituting the result into eqn. (12) leads to the macroscopic constitutive relation between the macroscopic stress $\bar{\sigma}$ and macroscopic strain $\bar{\epsilon}$. Clearly, appropriate choices of the forces F_N , F_T , and F_V can be considered in order to set to zero some components of the stress.

The in-plane mechanical properties of the lattice with extensional springs are:

- Poisson's ratio

$$\nu_L = \frac{\bar{\sigma}_{22} \bar{\epsilon}_{11} - \bar{\sigma}_{11} \bar{\epsilon}_{22}}{\bar{\sigma}_{11} \bar{\epsilon}_{11} - \bar{\sigma}_{22} \bar{\epsilon}_{22}} = \frac{d_1 \alpha_1^3 - 3\alpha_1^2 \alpha_2 + d_2 \alpha_1 \alpha_2^2 + d_3 \alpha_1^2 + d_4 \alpha_2^2 + d_5 \alpha_1 \alpha_2 + d_6 \alpha_1 + d_7 \alpha_2}{-d_1 \alpha_1^3 + d_8 \alpha_1^2 \alpha_2 + 3d_2 \alpha_1 \alpha_2^2 + d_9 \alpha_1^2 + 3d_4 \alpha_2^2 + d_{10} \alpha_1 \alpha_2 - d_6 \alpha_1 - d_7 \alpha_2} \quad (14)$$

where:

$$\begin{aligned} d_1 &= -9 \cos^4 \gamma \\ d_2 &= \sin^4 \gamma \\ d_3 &= 9(\cos^6 \gamma - 4 \cos^4 \gamma + 2 \cos^2 \gamma - 1) \\ d_4 &= \sin^4 \gamma \cos^2 \gamma \\ d_5 &= 3(6 \cos^4 \gamma - 7 \cos^2 \gamma - 2 \cos^6 \gamma + 1) \\ d_6 &= -9 \cos^2 \gamma \\ d_7 &= -3 \cos^2 \gamma \\ d_8 &= 3(4 \sin^2 \gamma \cos^2 \gamma + 1) \\ d_9 &= 9(3 \cos^6 \gamma - 4 \cos^4 \gamma + 2 \cos^2 \gamma + 1) \\ d_{10} &= 3(10 \cos^4 \gamma - 6 \cos^6 \gamma - 5 \cos^2 \gamma + 3) \end{aligned} \quad (15)$$

- Bulk modulus

$$K_L = \frac{1}{2} \frac{\bar{\sigma}_{11} + \bar{\sigma}_{22}}{\bar{\epsilon}_{11} + \bar{\epsilon}_{22}} = \frac{\sqrt{3} \sin^2 \gamma k_L}{2(\cos^2 \gamma + \alpha_1)} \quad (16)$$

- Young's modulus



$$E_L = \frac{\bar{\sigma}_{11}^2 - \bar{\sigma}_{22}^2}{\bar{\sigma}_{11}\bar{\epsilon}_{11} - \bar{\sigma}_{22}\bar{\epsilon}_{22}} = 2K_L(1-\nu) = \frac{2\sqrt{3}(9\cos^4\gamma\alpha_1^2 + \sin^4\gamma\alpha_2^2 + 3(2\cos^2\gamma\sin^2\gamma + 1)\alpha_1\alpha_2 + 9\alpha_1 + 3\alpha_2)\sin^2\gamma k_L}{-d_1\alpha_1^3 + d_8\alpha_1^2\alpha_2 + 3d_2\alpha_1\alpha_2^2 + d_9\alpha_1^2 + 3d_4\alpha_2^2 + d_{10}\alpha_1\alpha_2 - d_6\alpha_1 - d_7\alpha_2} \quad (17)$$

where the constants d_1, d_2, d_4, d_{6-10} are given in Eq. (15).

- Shear modulus

$$\mu_L = \frac{1}{2} \frac{\bar{\sigma}_{11} - \bar{\sigma}_{22}}{\bar{\epsilon}_{11} - \bar{\epsilon}_{22}} = \frac{1-\nu}{1+\nu} K_L = \frac{\sqrt{3}(9\cos^4\gamma\alpha_1^2 + \sin^4\gamma\alpha_2^2 + 3(2\cos^2\gamma\sin^2\gamma + 1)\alpha_1\alpha_2 + 9\alpha_1 + 3\alpha_2)\sin^2\gamma k_L}{12\cos^2\gamma\alpha_1^2\alpha_2 + 4\sin^2\gamma\alpha_1\alpha_2^2 + 9\sin^2 2\gamma\alpha_1^2 + 6(2 - \sin^2 2\gamma)\alpha_1\alpha_2 + \sin^2 2\gamma\alpha_2^2} \quad (18)$$

When rotational springs are considered the effective constants are as follows:

- Poisson's ratio

$$\nu_R = \frac{e_1\alpha_3^2 + e_2\alpha_4^2 + e_3\alpha_3\alpha_4 + e_4\alpha_3 + e_5\alpha_4}{e_6\alpha_3^2 + e_7\alpha_4^2 + e_8\alpha_3\alpha_4 - e_4\alpha_3 - e_5\alpha_4} \quad (19)$$

where:

$$\begin{aligned} e_1 &= 9(2\cos^4\gamma - 3\cos^2\gamma + 1) \\ e_2 &= (2\cos^4\gamma - \cos^2\gamma) \\ e_3 &= 3(4\cos^2\gamma \sin^2\gamma - 1) \\ e_4 &= 27\cos^2\gamma \\ e_5 &= 9\cos^2\gamma \\ e_6 &= 9(2\cos^4\gamma - \cos^2\gamma - 1) \\ e_7 &= 2\cos^4\gamma - 3\cos^2\gamma \\ e_8 &= 12\cos^2\gamma \sin^2\gamma - 9 \end{aligned} \quad (20)$$

- Bulk modulus

$$K_R = \frac{3\sqrt{3}(k_R / p^2)}{2(3\sin^2\gamma\alpha_3 + \cos^2\gamma\alpha_4 + 9\cos^2\gamma)} \quad (20)$$

- Young's modulus

$$E_R = \frac{6\sqrt{3}(3\alpha_3 + \alpha_4)(k_R / p^2)}{e_6\alpha_3^2 + e_7\alpha_4^2 + e_8\alpha_3\alpha_4 - e_4\alpha_3 - e_5\alpha_4} \quad (21)$$

- Shear modulus

$$\mu_R = \frac{3\sqrt{3}(3\alpha_3 + \alpha_4)(k_R / p^2)}{9\sin^2 2\gamma\alpha_3^2 + \sin^2 2\gamma\alpha_4^2 + 6(2 - \sin^2 2\gamma)\alpha_3\alpha_4} \quad (22)$$

ANALYSIS OF EFFECTIVE PROPERTIES

We analyze now the effective properties of the microstructured media. We consider the case of vanishing stiffness of the springs $k_L, k_R \rightarrow 0$. We have that:



$$\begin{aligned}
 \nu^* &\cong -1 + \nu_1^* k_{L,R}^* + O(k_{L,R}^2) \\
 K^* &\cong 0 + K_1^* k_{L,R}^* + O(k_{L,R}^2) \\
 E^* &\cong 0 + E_1^* k_{L,R}^* + O(k_{L,R}^2) \\
 \mu^* &\cong \mu_0^* + \mu_1^* k_{L,R}^* + O(k_{L,R}^2)
 \end{aligned}
 \tag{23}$$

where the coefficient ν_1^* , K_1^* , E_1^* , $\mu_0^* > 0$ are shown in Tab. 1.

Longitudinal spring	Rotational spring
$\nu_1^* = \frac{4p}{3} \frac{\eta_2 \eta_3}{EAEJ\eta_1} \tan^2 \gamma$	$\nu_1^* = \frac{4}{9} \frac{\eta_2 \eta_3}{EAEJ\eta_1 \cos^2 \gamma} \tan^2 \gamma$
$K_1^* = \frac{\sqrt{3}}{2} \tan^2 \gamma$	$K_1^* = \frac{\sqrt{3}}{6p^2 \cos^2 \gamma}$
$E_1^* = 2\sqrt{3} \tan^2 \gamma$	$E_1^* = \frac{2\sqrt{3}}{3p^2 \cos^2 \gamma}$
$\mu_0^* = \frac{3\sqrt{3}}{4p} \frac{EAEJ\eta_1}{\eta_2 \eta_3}$	$\mu_0^* = \frac{3\sqrt{3}}{4p} \frac{EAEJ\eta_1}{\eta_2 \eta_3}$

Table 1: Explicit expression of the coefficients in the asymptotic formulae in eqn. (23). In the table $\eta_1=3EJ+p^2EA$, $\eta_2=3EJ\sin^2\gamma+p^2EA\cos^2\gamma$, $\eta_3=3EJ\cos^2\gamma+p^2EA\sin^2\gamma$.

It is shown in (23) that also for deformable structures the Poisson's ratio remains -1 when the stiffness of the springs is zero, while the effect of the springs is to increase the value of ν^* . In such a limit, the bulk and the Young's moduli vanish while the shear modulus remains finite. The limiting behavior described in (23) can also be understood in term of relative stiffness between the spring elements and the elements of the lattice as described by the coefficients $\alpha_{1,\dots,4}$. In this respect, when $\alpha_{1,\dots,4} \rightarrow 0$, the same outcomes of eqns. (23) are obtained.

The dependence of the Poisson's ratio on the stiffnesses k_L and (k_R/p^2) is shown in Fig. 6. Results confirm that the Poisson's ratio approaches -1 when the spring constants are zero. It is worthwhile to mention the maximum theoretical values that can be reached by the Poisson's ratios at the limit $k_L, k_R/p^2 \rightarrow \infty$; the limiting expressions are:

$$\begin{aligned}
 \nu^* &\cong \frac{1}{3} - \frac{1 + \sin^2 \gamma \cos^2 \gamma}{\sin^2 \gamma} \left(\frac{s}{p} \right)^2 + O((s/p)^4) \\
 \nu^* &\cong \frac{1 - 2 \cos^2 \gamma}{3 - 2 \cos^2 \gamma} \left(1 - \frac{(s/p)^2}{3 - 2 \cos^2 \gamma} \right) + O((s/p)^4)
 \end{aligned}
 \tag{24}$$

where we have considered, for simplicity, rectangular cross-sections of the arms, so that $A=ts$ and $J=ts^3/12$, where s and t are the in-plane and out-of-plane thicknesses, respectively. In the following Fig. 6 we compare the effective Poisson's ratio ν^* of the triangular lattice in function of the stiffness of the longitudinal springs k_L , see Fig. 6a, and in function of the slenderness $\lambda=p/s$ of the arms, see Fig. 6b. In each figure we consider three different materials with Young's modulus $E=3000$ MPa for thermoplastic polymer (ABS), $E=60000$ MPa for granite and $E=200000$ MPa for steel, the geometric configuration considered is given by the angle $\gamma=4\pi/9$. All the computations are performed considering a thickness t of the lattice out of plane of 1 mm. In Fig. 6a we have considered arms with length $p=50$ mm and in-plane thickness $s=10$ mm. In Fig. 6b the values of the Poisson' ratio are significant when $\lambda=p/s \geq 5$, in the range of validity of the beam theory which has been used for the computation of the effective behavior, anyway we show with dotted line the values of the Poisson' ratio even for $\lambda < 5$. The value of the stiffness of the springs has been set equal to $k_L=1$ N/mm. As it is possible to see in Fig. 6, when the contribution of the spring is less relevant the Poisson's ratio approaches -1, as confirmed by



analytical formulae, both when the stiffness of the spring $k_L \rightarrow 0$, and when the slenderness of the arms $\lambda \rightarrow 0$. On the contrary when the stiffness of the springs is big the Poisson's ratio approaches $1/3$, as in the case of the classical triangular lattice used in several physical models and engineering.

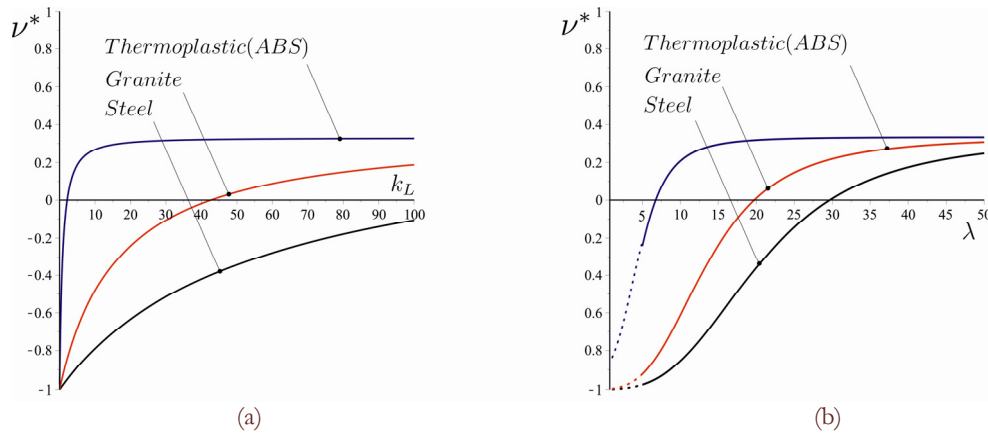


Figure 6: Effective Poisson's ratio ν^* for three different materials in the case of longitudinal springs. (a) Poisson's ratio as a function of the stiffness k_L . (b) Poisson's ratio as a function of the slenderness $\lambda = p/s$.

In the Fig. 7 we show the same results in the case of the lattice with rotational springs, for which the same considerations of the previous case are still valid.

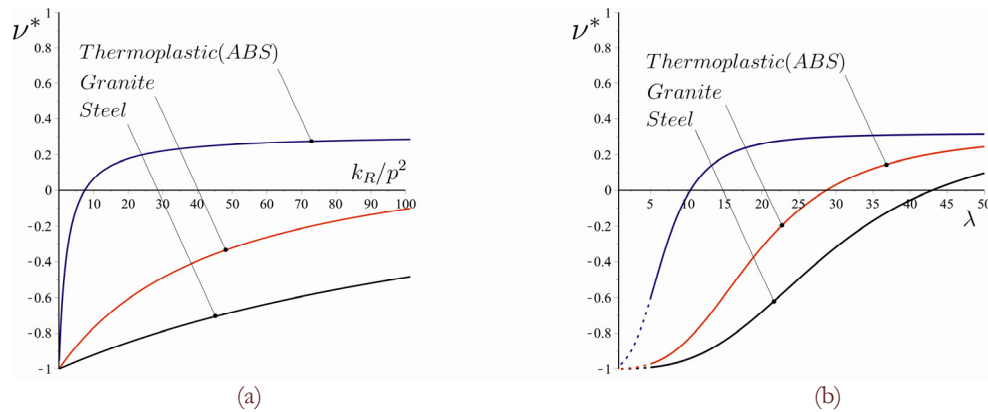


Figure 7: Effective Poisson's ratio ν^* for three different materials in the case of rotational springs. (a) Poisson's ratio as a function of the stiffness k_R/p^2 . (b) Poisson's ratio as a function of the slenderness $\lambda = p/s$.

CONCLUSIONS

The constitutive properties of a new auxetic material are obtained analytically by using classical beam theory in the analysis of the microstructure of the lattice. Results show that the effective Poisson's ratio of the lattice is arbitrarily close to -1.

ACKNOWLEDGMENTS

M.B. acknowledges the financial support of the European Community's Seven Framework Programme under contract number PIEF-GA-2011-302357-DYNAMETA and of Regione Autonoma della Sardegna (LR7 2010, grant 'M4' CRP-27585).



REFERENCES

- [1] Gibson, L.J., Ashby, M.F., Schajer, G.S., Robertson, C.I., The mechanics of two dimensional cellular solids, In: Proc. R. Soc. Lond. A, 382 (1982) 25-42.
- [2] Prall, D., Lakes, R.S., Properties of a chiral honeycomb with a Poisson's ratio of $\nu=-1$, *Int. J. Mech. Sci.*, 39 (1997) 305-307, 309-314.
- [3] Spadoni, A., Ruzzene, M., Elasto-static micropolar behavior of a chiral auxetic Lattice, *J. Mech. Phys. Solids*, 60 (2011) 156-171.
- [4] Wojciechowski, K.W., Two-dimensional isotropic system with a negative Poisson ratio Elasto-static micropolar behavior of a chiral auxetic lattice, *Physics Letters A*, 137 (1989) 60-64.
- [5] Bathurst, R.J., Rothenburg, L., Note on a random isotropic granular material with negative Poisson's ratio, *Int. J. Eng. Sci.*, 26 (1988) 373-383.
- [6] Caddock, B.D., Evans, K.E., Microporous materials with negative Poisson's ratios, I. Microstructure and mechanical properties, *J. Phys. D: Appl. Phys.*, 22 (1989) 1877-1882.
- [7] Webber, R. S., Alderson, K. L., Evans, K.E., A novel fabrication route for auxetic polyethylene Part 2: mechanical properties, *Polym. Eng. Sci.*, 48-7 (2008) 1351-1358.
- [8] Lakes, R.S., Elms, K.E., Indentability of conventional and negative Poisson's ratio foams, *J. Compos. Mater.*, 27-12 (1993) 1193-1202.
- [9] Chan, N., Evans, K. E., Indentation resilience of conventional and auxetic foams, *J. Cell. Plast.*, 34 (1998) 231-260.
- [10] Lakes, R.S., Foam structure with a negative Poisson's ratio, *Science*, 235 (1987) 1038-1040.
- [11] Burke, M., A stretch of the imagination, *New Scientist*, 154-2085 (1997) 36-39.
- [12] Chen, C. P., Lakes, R. S., Dynamic wave dispersion and loss properties of conventional and negative Poisson's ratio polymeric cellular materials, *Cell. Polym.*, 8-5 (1989) 343-369.
- [13] Scarpa, F., Dallochio, F., Ruzzene, M., Identification of acoustic properties of auxetic foams, *Smart Struct. Mater.: Damping Isol.*, 5052 (2003) 468-474.
- [14] Ruzzene, M., Vibration and sound radiation of sandwich beams with honeycomb truss core, *J. Sound Vib.*, 277-4-5 (2004) 741-763.
- [15] Patel, J., Ananthasuresh, G.K., A kinematic theory for radially foldable planar linkages, *Int. J. Solids Struct.*, 44 (2007) 6279-6298.
- [16] Cabras, L., Brun, M., Auxetic two-dimensional lattice with Poisson's ratio arbitrarily close to -1, submitted.
- [17] Kittel, C., *Introduction to Solid State Physics*, seventh ed., John Wiley & Sons, New York, (1996).